HHS Public Access

Author manuscript

Anal Chem. Author manuscript; available in PMC 2018 November 07.

Published in final edited form as:

Anal Chem. 2017 November 07; 89(21): 11758–11764. doi:10.1021/acs.analchem.7b03336.

Rapid Enrichment and Sensitive Detection of Multiple Metal Ions Enabled by Macroporous Graphene Foam

Xiaoni Fang[1], **Yang Liu**[1], **Luis Jimenez**[1], **Yaokai Duan**[1], **Gary Brent Adkins**[1], **Liang Qiao**[2], **Baohong Liu**[2], and **Wenwan Zhong**[1,*]

[1]Department of Chemistry, University of California, Riverside, 92521 CA

[2]Department of Chemistry, Institute of Biomedical Sciences and State Key Lab of Molecular Engineering of Polymers, Shanghai Stomatological Hospital, Fudan University, Shanghai 200433, China

Abstract

Nanomaterials have shown great promises in advancing biomedical and environmental analysis because of the unique properties originated from their ultrafine dimensions. In general, nanomaterials are separately applied to either enhance detection by producing strong signals upon target recognition; or to specifically extract analytes taking advantage of their high specific surface area. Herein, we report a dual-functional nanomaterial-based platform that can simultaneously enrich and enable sensitive detection of multiple metal ions. The macroporous graphene foam (GF) we prepared display abundant phosphate groups on the surface and can extract divalent metal ions via metal-phosphate coordination. The enriched metal ions then activate the metal-responsive DNAzymes and produce the fluorescently labeled single-stranded DNAs that are adsorbed and quenched by the GF. The resultant fluorescence reduction can be used for metal quantitation. The present work demonstrated duplexed detection of Pb^{2+} and Cu^{2+} using the Pb and Cu-responsive DNAzymes, achieving a low detection limit of 50 pM and 0.6 nM, respectively. Successful quantification of Pb^{2+} and Cu^{2+} in human serum and river water were achieved with high metal recovery. Since the phosphate-decorated GF can enrich diverse types of divalent metal cations, this dual-functional GF-DNAzyme platform can serve as a simple and cost-effective tool for rapid and accurate metal quantification in determination of human metal exposure and inspection of environmental contamination.

Graphical Abstract

*Corresponding Author: wenwan.zhong@ucr.edu; Fax: +1-951-827-4713.

Notes

The authors declare no competing financial interest.

Supporting Information

Adsorbed amount of metal ions and DNA by GF at different conditions, recoveries of Pb^{2+} and Cu^{2+} at low concentrations after enriched by GF, comparison of fluorescence spectra of Cy3-ssDNA and Cy3-dsDNA with and without GF, influence of different buffer on the quenching efficiency of GF, fluorescence quenching efficiency by different material, determination of Cu^{2+} and Pb^{2+} in environmental water and plasma sample were listed in supplementary information. This material is available free of charge via internet at http://pubs.a.org/.

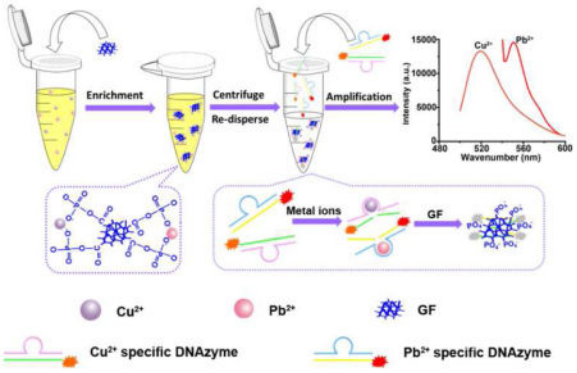

Heavy metals such as copper and lead are continuously released to our environment through industrial and human activities like gasoline processing, electronic waste disposal, fertilizer usage, etc.[1–3] They are difficult to be degraded and make their ways to plants and living organisms, imposing persistent risk to our ecosystems. Metal pollution in the environment also represents a great threat to human beings, because they could cause severe health issues like memory loss, blindness and deafness, kidney damage, cancers, etc.[4–6] In particular, childhood exposure to lead can damage learning and recognition capabilities for the entire life-time; and copper can induce the pathogenesis of hepatic disorder, neurodegenerative changes and other disease conditions.[7–9] Thus, it is of paramount importance to constantly survey heavy metal contents in environmental samples as well as in clinical specimen for pollution reduction and human exposure prevention.

With the acute toxicity of single heavy metals well documented, safety guidelines and regulations are established for individual metals in water, sediment or other environmental subjects. However, little progress has been made to evaluate the impact of metal mixture in the environment.[10–12] Metals in the mixture would compete or share binding sites to biological receptors, leading to different toxicity and uptake behaviors than single metals.[13,14] The high complexity of the metal mixtures found in the environment and its potentially enhanced danger to the ecosystem and human health call for simple survey techniques that can detect multiple metals selectively and sensitively in a fast and high-throughput manner.

Detection of metal mixtures in complex biological or environmental samples demands higher sensitivity and selectivity compared to single metal detection. Electrochemical sensors have been developed for measurement of heavy metals, but with poor discrimination capability and low sensitivity.[15–18] Mass spectrometric and optical spectroscopic methods are still the main approaches for assessment of metal mixtures in the environment, which include flame atomic absorption spectroscopy (FAAS), electrothermal atomic absorption spectroscopy (ETAAS), inductively coupled plasma optical emission spectroscopy (ICP-OES), and ICP-mass spectrometry (MS). While such instrumental analysis permit very sensitive and simultaneous detection of a large numbers of metals, they are expensive, take up a lot of space, and require well-trained scientists to operate, making it difficult for on-site and real-time detection.[19,20] New methods for detection of metal mixtures are desired for field-survey of environmental contamination and point-of-care applications.

Our approach to overcome the aforementioned problems is to combine the high selectivity of the metal-responsive DNAzymes and the strong absorptivity of nanomaterials in designing sensors for ultrasensitive and multiplexed metal detection. Metal-responsive DNAzymes have been discovered by systematic evolution of ligands by exponential enrichment (SELEX), showing good catalytic ability and binding activity towards many specific metal ions.[21–23] Nanomaterials, with judicious design, can provide large specific surface areas and tunable functional groups to facilitate metal ion absorption. They could also possess superior optical property or quenching capability to enable sensitivity and simple fluorescent or colorimetric detection. Herein, we constructed our sensor by combing the macroporous graphene foam (GF) with the Cu- and Pb-specific DNAzymes for simultaneous enrichment and detection of Cu^{2+} and Pb^{2+} from aqueous solutions. The GF acts as both an extractor for metal ions and a quencher for the fluorophores that label the DNAzymes (Scheme 1). The dual functionality comes from the phosphate groups on the GF surface that can coordinate with the metal cations for their extraction; and the graphene backbone that can bind to single-stranded DNA (ssDNA) strongly and quench the fluorophores attached to the ssDNAs. Once Cu^{2+} and Pb^{2+} are enriched on the surface of GF, they can activate the corresponding DNAzymes and release the ssDNA products that are linked to two different fluorophores. The turn-off fluorescence from the released fluorophores then allows quantitative measurement of the contents of these two metals simultaneously. Sensitive detection of Pb^{2+} and Cu^{2+} in serum and environmental water samples were attained in the present work.

EXPERIMENTAL SECTION

Chemicals

The Pb^{2+}-specific DNAzyme (Pb-Sub: 5′-/5Cy3/ACT CAC TAT rAGG AAG AGA TG -3′ and Pb-Enz: 5′-CAT CTC TTC TCC GAG CCG GTC GAA ATA GTG AGT-3′) and the Cu^{2+}-specific DNAzyme (Cu-Sub: 5′-TTT TTT TTT TAG CTT CTT TCT AAT ACrG GCT TAC C/36-FAM/-3′ and Cu-Enz: 5′-GGT AAG CCT GGG CCT CTT TCT TTT TAA GAA AGA AC-3′) were synthesized and purified by Integrated DNA Technologies, Inc. (IDT) (Coralville, IA). Graphene oxide (GO), phytic acid (PA), Tris base and ascorbic acid (AA) were obtained from Sigma-Aldrich (St. Louis, MO). Cupric nitrate ($Cu(NO_3)_2$, 99%), lead acetate ($Pb(CH_3COOH)_2$, ≥98.0%), manganese nitrate ($Mn(NO_3)_2$, 99%), magnesium nitrate ($Mg(NO_3)_2$, 99%), cadmium nitrate ($Cd(NO_3)_2$, 99%), nickel nitrate ($Ni(NO_3)_2$, 99%), cobalt nitrate ($Co(NO_3)_2$, 99%), ferric nitrate ($Fe(NO_3)_3$, > 98.0%), zinc nitrate ($Zn(NO_3)_2$, 99%), magnesium chloride ($MgCl_2$, 99%), potassium chloride (KCl, 99%), nitric acid (HNO_3,) were purchased from Fisher Scientific (Waltham, MA). All the reagents were used as received without further purification. All experiments and measurements were carried out at room temperature unless otherwise stated. Deionized water (18.4 MΩ) used for all experiments was obtained from a Milli-Q system (Millipore, Bedford, MA).

Synthesis and characterization of GF

Graphene foam (GF) was prepared by using phytic acid as the gelator and dopant and Graphene oxide (GO) was employed as the precursor, as reported by Chen *et al.*[24] Briefly, 0.5 mL of PA was added into 15 mL of GO (2 mg/mL, aqueous solution) and sonicated for

40 min at room temperature. Then, the mixture was sealed in a 25-mL Teflon-lined autoclave tube and maintained at 180 °C for 12 h. Subsequently, the solid precipitate formed from the reaction was collected by tweezer after the autoclave tube was naturally cooled to room temperature. The product was washed by ethanol and water, and then freeze-dried for 24 h to obtain the desired final product, GF.

Transmission electron microscopy (TEM) images were directly taken with a JEOL 2011 microscope operated at 200 kV (JEOL, Tokyo, Japan). Samples were suspended in ethanol and spotted on a carbon-coated copper grid. The infrared spectra were obtained by using a FTIR 360 manufactured by Ni-colet (Thermofisher, USA). X-ray photoelectron spectroscopy (XPS) data were collected by an X-ray photoelectron spectrometer (PerkinElmer PHI 5000C ESCA System) equipped with Mg Kα radiation. Raman spectra were taken by a Labram-1B Raman spectrometer from Yobin Yvon with a laser (2 mW) excitation wavelength of 632.8 nm.

Preparation of DNAzymes

Equimolar of the enzyme strand and the Cy3 or AFM labelled substrate strand were added into the reaction buffer (50 mM $MgCl_2$ and 5 mM Tris, pH ~ 8.0) and denatured at 98 °C for 2 min in a water bath. The obtained DNAzymes were stored at 4 °C after cooled to room temperature.

Detection of metal ions based on GF

The procedure for extraction and detection of metal ions based on GF is shown in Scheme 1. For metal ion extraction, 20 μg of GF was added into 1 mL of the metal solution at different metal cation concentrations in 0.5 M of KCl-HCl (pH 1.5). The solution was stirred at room temperature for 30 min to reach maximum adsorption, and then the solution was centrifuged. After removal of the supernatant, the GF was re-suspended in $MgCl_2$-Tris buffer (50 mM $MgCl_2$ and 50 mM Tris, pH ~ 8.0, 90 μL), followed by addition of both DNAzymes reaching a final concentration of 5 nM. Then, 5 L of AA (5 mM) was supplied to reduce Cu^{2+} to Cu^{+} and incubated for 10 minutes at room temperature. Subsequently, solution fluorescence was measured as described in Fluorescence Measurement. Detection of metal contents in serum and environmental water samples were carried in the same manner.

ICP-AES analysis

The Optima 200DV Inductively Coupled Plasma - Atomic Emission Spectrometer (ICP-AES) (Perkin Elmer, Norwalk, CT) was employed to verify the quantities of all metals recovered from the standard metal solutions and the unknown samples. The samples were acidified with 10% HNO_3 before analysis. The instrument was rinsed thoroughly with 10% HNO_3 before injection to prevent memory effects. The argon source (> 99%) was set at 90 psi. The data was acquired using the ICP Expert II software. A blank was run at the beginning of each measurement to establish the baseline level. Then, standard solutions and unknown samples were measured in triplicate. A standard curve was generated to determine the concentration of the unknown samples.

Fluorescence measurements

Fluorescence measurements were conducted on a QM400 fluorometer (HORIBA, Japan). For detection of Pb^{2+} with the Cy3 labeled Pb-specific DNAzyme, the excitation and emission wavelengths (λ_{Ex} and λ_{Em}) were set at 535 and 540–600 nm, respectively. Copper detection was performed with the $\lambda_{Ex}/\lambda_{Em}$ at 496 nm/500–600 nm that detected the FAM label on the Cu-specific DNAzyme. The slit width for both excitation and emission was set at 5 nm. One hundred μL sample was added to the cuvette and the fluorescence spectra were scanned. The cuvette was washed with pure water for three times and dried under N_2 after each sample.

RESULTS AND DISCUSSION

Characterization of GF

GF was prepared from GO by a thermal annealing approach using phytic acid (PA) as the gelator and dopant.[24] PA not only reduced the GO sheets and assembled them into the compact, highly porous foam with good structural stability, but also introduced many phosphate groups onto the GO surface. As shown in the SEM image in Figure 1a, the pore size of GF was ~10 μm in diameter. The finer structure revealed by TEM (Figure 1b) illustrates the wrinkled and even folded layers of GF. Thus, GF is like a sponge containing rough surface and pores that provide high absorptivity for target compounds and rapid diffusion for the absorbed molecules. The elemental composition of GF was probed by XPS. All of the binding energies in XPS spectra were calibrated using the carbonaceous C1s line (284.6 eV) as the reference. Figure 1c reveals a graphitic C1s peak at around 284.8 eV, a strong O1s peak at around 532.7 eV, and the characteristic P2s and P2p peaks at 191 and 134.5 eV. These peaks confirm the presence of the hydrophilic oxygen-containing groups, such as the hydroxyl/epoxyl groups on GF surface, as well as prove the successful integration of PA. XPS elemental analysis also supports the rich content of C, O, and P in the material. (Figure 1d).

Chemical modification with PA on the GF was further validated by FT-IR and Raman spectroscopy. The spectra of the GF were compared with that of the GO to illustrate the key differences between these two materials. As shown in Figure 2a, both GO and GF exhibit the C=C bond stretch at 1615 and 3415 cm^{-1} when examined by FT-IR. The spectrum for GF also contains the distinct transmittance peaks at 1161, 1057, 1003, and 886 cm^{-1} which can be ascribed to the stretching vibrations of P=O, P-O-C (phosphate ester group), P-O, and P-O-H, respectively. The peak at 510 cm^{-1} can be assigned to the de-formation vibration of PO_4. The Raman spectra reveal the typical G band at about 1580 cm^{-1}, and the D band at about 1340 cm^{-1} for both GO and GF (Figure 2b). The ratio of the intensities of the D and G bands (ID/IG) can be utilized to judge the degree of structural disorder and defects. The relatively large amounts of phosphate groups originating from PA reduce the relative number of the six-membered aromatic rings, and thus increase the degree of structural disorder: the ratio of ID/IG was enlarged by 10% compared to that of GO.

GF for metal ion enrichment

The above examination results prove that macroporous GF was successfully synthesized. The prepared GF not only holds the basic structure of GO but also contained abundant phosphate groups on the surface. The phosphate groups can form strong coordination with transition metals, and the conjugated carbon structure on GF surface can establish the cation-π interaction with the metal ions, both making GF an excellent sorbent for metals. To test this, Pb^{2+} and Cu^{2+}, the contents of which should be monitored closely in the environment and exposure patients, were chosen as the model cations for optimization of the adsorption conditions by GF. After 30 min incubation of Pb^{2+} and Cu^{2+} at different pH values (from 0.5 – 2.5) and salt conditions (0.05 – 2.0 M KCl-HCl, as well as 0.05 M of PA-HCl and glycine-HCl), the adsorption reached the maximum values in 0.5 M KCl-HCl buffer (pH~1.5) for both Pb^{2+} and Cu^{2+} (Figure S1, Supporting Information). The low pH in this buffer can ensure all metals are soluble, and the high salt content is needed for the latter steps involved DNAzymes. Moreover, we tested adsorption of diverse transition metal cations, Cd^{2+}, Zn^{2+}, Mn^{2+}, Co^{2+}, Mg^{2+}, Ni^{2+}, Pb^{2+} and Cu^{2+} on the GF in the optimal buffer. As shown in Figure 3a, more than 90% of the added metal ions were enriched by GF within 30 min. In particular, Pb^{2+} and Cu^{2+} exhibited the fastest adsorption rates, reaching the adsorption maximum of 92% and 96% within 120 min. The adsorption capacity was also examined at the extended incubation period of 120 min. Most of the metals, including Cu^{2+}, can reach the maximum capacity, q_{max}, of 15–50 mg of metal per gram of GF (46.3±0.9, 35.7±1.8, 24.1±3.3, 21.5±0.5, 13.1±2.5, 29.1±4.3, and 27.8±2.6 mg/g GF for Cd^{2+}, Zn^{2+}, Mn^{2+}, Pb^{2+}, Co^{2+}, Mg^{2+}, Ni^{2+}, and Cu^{2+}, respectively), but the q_{max} of Pb^{2+} was 97.4±0.6 mg/g GF, more than 3 times higher than others. For both Pb^{2+} and Cu^{2+}, we tested the recoveries at various metal concentrations. We found that even with lower than 1 mg/L of the metal ion, at which concentration the adsorption efficiency would be limited by the concentration-driven diffusion to the surface of GF, the recovery was more than 80% (Figure S2, Supporting Information). All of the above results confirm that GF can rapidly capture and concentrate trace metal ions. The enrichment should benefit sensitive detection of trace metals in samples.

Construction of the GF sensor for the detection of metal ions

Besides its large specific area functionalized with groups beneficial for metal enrichment, GF contains the graphene structure that can help with *in situ* detection of the enriched ions. It has been well studied that single-stranded DNA (ssDNA) can bind strongly to graphene via π-π stacking between the bases on nucleotides and the sp^2-hybridized carbon atoms in the extended π-conjugation on graphene. In particular, guanine (G) shows enhanced binding via the NH-π interaction, supported by both computational simulation and experimental measurement.[25,26] As shown in Figure S3 (Supporting Information), DNA can be adsorbed by GF within 10 min, with the maximum capacity reaching 11.6 mg DNA $(g\ GF)^{-1}$. In addition, the planar carbon π system on graphitic domain can establish long range resonance energy transfer with the adsorbed dye molecules, quenching a wide range of fluorophores with high efficiency.[27,28] Based on these features, we designed our metal sensor by coupling the porous GF with the fluorescently labeled, metal-responsive DNAzymes: the enriched metals on the GF surface can specifically cleave the substrate of the DNAzyme, and the cleaved product would be subsequently adsorbed and quenched by the GF.

Diverse DNAzymes have been reported for metal sensing.[29–31] Thus, the two DNAzymes specific for Pb^{2+} and Cu^{2+} were chosen, and the substrate strands were labeled with Cy3 and FAM, respectively. The fluorophores were not quenched by GF when the DNAzymes were intact, owing to the double-stranded regions formed between the substrate and enzyme strands. Once the DNAzymes were mixed with the Pb^{2+} or Cu^{2+} enriched by GF, the substrate strand was cleaved and the released ssDNA was adsorbed and the fluorophore was quenched by GF. As shown in Figure S4 (Supporting Information), the 100 nM Cy3-labeled ssDNA product resulted from the Pb-induced substrate cleavage could be quenched completely by 20 μg/mL of GF, while the fluorescence of the intact DNAzyme was not affected by the presence of GF. TEM was used to examine the GF before and after metal enrichment and DNAzyme cleavage, and revealed no difference on the GF (Figure S5, Supporting Information). The presence of GF did not affect the cleavage efficiency, as proved by using gel electrophoresis to monitor product generation with or without GF (Figure S5c).

Since the salt content, concentration, and pH value of the reaction buffer could influence the structure stability of the DNAzymes and interaction between DNA and GF, we compared the quenching efficiency of GF in three kinds of common buffers (50 mM NaCl in 50 mM phosphate buffer at pH 7.4; 50 mM $MgCl_2$ in 50 mM Tris buffer at pH 8.0; and 50 mM $NaNO_3$ in 50 mM Tris-Acetate at pH 7.8). The quenching efficiency was defined as $(F_0 - F)/F_0$, where F and F_0 are the fluorescence intensities of the DNA solutions with and without the presence of the nanomaterial, respectively. As shown in Figure S6 (Supporting Information), these buffers showed similar quenching efficiency with GF. We chose the $MgCl_2$-Tris buffer because it exhibited better quenching stability in repeated measurements. We also compared the quenching capability of GF with other common graphene materials: graphene (G), graphene oxide (GO), and the hydrophobic macroporous graphene foam (MGF), in this buffer (Figure S7, Supporting Information). The signals were measured at 30 min after the metal ion, nanomaterials, and the DNAzyme were mixed. While fixing the concentrations of the DNAzyme and the metal ions in the mixture, the quenching efficiency increased linearly with the increase of GF concentration until reaching a plateau (larger than 90%) at around 40 μg/mL. On contrary, the other materials showed similar trends but with much slower rates of increase; and no plateau was attained even with 200 μg/mL of the material used. The higher quenching efficiency exhibited by GF compared to the other graphene-based materials could be attributed: (I) the inherent aromatic structure and amphiphilic property of GF; and (II) the increased structural disorder and defects of GF. The former feature facilitates highly efficient adsorption of ssDNA; and the latter benefits long-range energy transfer and results in enhanced quench of fluorescence.[32–34] Moreover, the adsorption event occurred very rapidly: within 5 min, the quenching efficiency of GF for ssDNA reached the maximum value of 98% (Figure S8, Supporting Information). The high quenching efficiency can help improve the signal-to-noise ratio of our sensing method; and prompt adsorption of the cleaved product can ensure fast detection upon metal enrichment, allowing us to perform sensitive and quick survey of these two toxic metals in samples of interest.

Performance of the GF sensor in the detection of metal ions

The performance of our GF-based metal sensor was examined. Figure 4a&c shows the fluorescence spectra of the sensing system upon enriching Pb^{2+} and Cu^{2+} from the 1-mL solution at various concentrations using the GF, followed with detection in the 100-μL DNAzyme solution. The fluorescence intensity decreased dramatically as the concentrations of Pb^{2+} increased. The limit of detection (LOD) was calculated to be 50 pM and 0.6 nM for Pb^{2+} and Cu^{2+}, respectively, using the 3σ method. These LODs are much lower than most of the previously reported approaches for Pb^{2+} and Cu^{2+} detection, as shown in Table 1 that compares the LODs of various techniques for Pb^{2+} and Cu^{2+} detection. The high sensitivity of our sensing system can be attributed to both the excellent metal enrichment capability of GF and its high quenching efficiency over the fluorescently labeled ssDNA. Furthermore, we evaluated the impact from Cu^{2+} to detection of Pb^{2+}, and vice versa. The fluorescence intensity change of the Pb-specific DNAzyme caused by incubation with the GF enriching 50 nM Pb^{2+} did not vary with the presence of Cu^{2+} ranging from 1×10^{-12} M to 1×10^{-4} M. Similarly, the coexistence of 1×10^{-12} M to 1×10^{-4} M Pb^{2+} did not affect the signal from 0.6 nM Cu^{2+} (Figure S9, Supporting Information).

We further tested whether other divalent metals could affect selective detection of Pb^{2+} and Cu^{2+}. The fluorescence response was monitored when the sensing system was challenged by the presence of other metal ions, including Mn^{2+}, Mg^{2+}, Cd^{2+}, Ni^{2+}, Co^{2+}, Fe^{2+}, Zn^{2+}. As shown in Figure 5, the GF sensor yielded much more quenching with 10 nM Pb^{2+} or Cu^{2+}, compared to that obtained with other metal ions at 100-fold higher concentrations. The excellent selectivity is originated from the high specificity of each DNAzyme to its target cation, as well as from the good capability of GF in differentiating ss- and ds-DNA.

Application of the GF sensor

The above results indicate the potential of our GF-DNAzyme sensing platform in extraction and detection of Pb^{2+} and Cu^{2+} present in complex biological and environmental systems. Most of metal ions exposure can be measured by testing ions concentration in serum.[44,45] To demonstrate this, we spiked Pb^{2+} and Cu^{2+} to the human serum obtained from Sigma, and detected their contents using our sensor. Each metal was spiked at two concentrations: 0.1 and 1.0 nM for Pb^{2+}; and 1.0 and 10.0 nM for Cu^{2+}. The metal concentration obtained with our sensing method was divided by the actual spiked concentration to achieve the recovery, which was presented in Table 2. The recoveries for both metal ions at the two concentrations tested were more than 95 ± 3%. Switching serum with plasma, low concentrations of Pb^{2+} and Cu^{2+} were still determined successfully with excellent recoveries using the developed approach (Table S2, Supporting Information).

Environmental water is another type of samples that could be subject to survey of heavy metal contamination (Table S1, Supporting Information). We collected some water samples from the Santa Ana River at ~100 meter downstream from the waste water treatment plant for City of Riverside. The river sample did not contain detectible level of Pb^{2+} or Cu^{2+}, indicating no heavy metal contamination in the discharged water from the treatment plant. If spiked with these two metal cations, the detected quantity agreed well with the true content. In human serum, plasma, and environmental water, the metal recovery found with our sensor

is similarly high, which indicates that sample viscosity has no obvious influence on our sensor. All the results support our GF-DNAzyme sensing system can be used to monitor Pb^{2+} and Cu^{2+} simultaneously with desirable sensitivity and accuracy in complex samples.

CONCLUSIONS

In summary, we present a simple method for quick, sensitive, and selective detection of metal ions using the macroporous GF. Taking advantage of the abundant phosphate groups on its surface, its high specific surface area, and the unique DNA adsorption and fluorophore quenching properties, the macroporous GF enables both metal ion extraction and fluorescence-based detection. The enrichment and detection can be completed within 1 hr; and multiple metals can be enriched simultaneously, with detection limits for specific metals such as Pb^{2+} and Cu^{2+} reaching the low nM or even pM range. The sensor is also tolerant to complex sample matrices, as demonstrated by metal quantification in serum, plasma, and environmental water, eliminating the need of sample pretreatment. With the availability of numerous DNAzymes specifically targeting different metals and fluorophores detectible at various wavelengths, our method can be expanded for multiplexed detection of several metal ions for quick and easy assessment of metal contents in environmental samples and medical specimens. It will be valuable for on-site survey of heavy metal contamination and for diagnosis of metal exposure in patients.

Supplementary Material

Refer to Web version on PubMed Central for supplementary material.

Acknowledgments

The authors would like to thank the National Institutes of Health for the support provided by R01 CA188991 to W.Z.

References

1. Tchounwou PB, Yedjou CG, Patlolla AK, Sutton DJ. EXS. 2012; 101:133–164. [PubMed: 22945569]
2. He ZL, Yang XE, Stoffella PJ. J Trace Elem Med Bio. 2005; 19:125–140. [PubMed: 16325528]
3. Järup L. Br Med Bull. 2003; 68:167–182. [PubMed: 14757716]
4. De Lurdes Dinis, M.Fiúza, A.Simeonov, LI.Ko-chubovski, MV., Simeonova, BG., editors. Springer Netherlands; Dord: 2011. p. 27-50.
5. Wuana RA, Okieimen FE. ISRN Ecology. 2011; 2011:20.
6. Singh R, Gautam N, Mishra A, Gupta R. Indian J Pharmacol. 2011; 43:246–253. [PubMed: 21713085]
7. Mason LH, Harp JP, Han DY. BioMed Res Int. 2014; 2014:840547. [PubMed: 24516855]
8. Zeliger HI. Interdis Toxicol. 2014; 7:117–122.
9. Gaetke LM, Chow-Johnson HS, Chow CK. Arch Toxicol. 2014; 88:1929–1938. [PubMed: 25199685]
10. Clement RE, Yang PW, Koester CJ. Anal Chem. 1999; 71:257–292.
11. Li L, Feng J, Fan Y, Tang B. Anal Chem. 2015; 87:4829–4835. [PubMed: 25853631]
12. Hwang K, Wu P, Kim T, Lei L, Tian S, Wang Y, Lu Y. Angew Chem Int Ed. 2014; 53:13798–13802.

13. Nys C, Versieren L, Cordery KI, Blust R, Smolders E, De Schamphelaere KAC. Environ Sci Technol. 2017; 51:4615–4623. [PubMed: 28339194]
14. Horner TJ, Lee RBY, Henderson GM, Rickaby REM. P Natl Acad Sci USA. 2013; 110:2500–2505.
15. Li D, Song S, Fan C. Acc Chem Res. 2010; 43:631–641. [PubMed: 20222738]
16. Shen L, Chen Z, Li Y, He S, Xie S, Xu X, Liang Z, Meng X, Li Q, Zhu Z, Li M, Le XC, Shao Y. Anal Chem. 2008; 80:6323–6328. [PubMed: 18627134]
17. Zhu Z, Su Y, Li J, Li D, Zhang J, Song S, Zhao Y, Li G, Fan C. Anal Chem. 2009; 81:7660–7666. [PubMed: 19691296]
18. Wu D, Zhang Q, Chu X, Wang H, Shen G, Yu R. Biosens Bioelectron. 2010; 25:1025–1031. [PubMed: 19819684]
19. Zhao XH, Kong RM, Zhang XB, Meng HM, Liu WN, Tan W, Shen GL, Yu RQ. Anal Chem. 2011; 83:5062–5066. [PubMed: 21639104]
20. Park M, Ha HD, Kim YT, Jung JH, Kim SH, Kim DH, Seo TS. Anal Chem. 2015; 87:10969–10975. [PubMed: 26456631]
21. Lee JH, Wang Z, Liu J, Lu Y. J Am Chem Soc. 2008; 130:14217–14226. [PubMed: 18837498]
22. Mazumdar D, Nagraj N, Kim HK, Meng X, Brown AK, Sun Q, Li W, Lu Y. J Am Chem Soc. 2009; 131:5506–5515. [PubMed: 19326878]
23. Zhang XB, Kong RM, Lu Y. Annual Review of Analytical Chemistry. 2011; 4:105–128.
24. Song X, Chen Y, Rong M, Xie Z, Zhao T, Wang Y, Chen X, Wolfbeis OS. Angew Chem Int Ed. 2016; 55:3936–3941.
25. Moraca F, Amato J, Ortuso F, Artese A, Pagano B, Novellino E, Alcaro S, Parrinello M, Limongelli V. P Natl Acad Sci USA. 2017; 114:E2136–E2145.
26. Georgakilas V, Tiwari JN, Kemp KC, Perman JA, Bourlinos AB, Kim KS, Zboril R. Chem Rev. 2016; 116:5464–5519. [PubMed: 27033639]
27. Britz DA, Khlobystov AN. Chem Soc Rev. 2006; 35:637–659. [PubMed: 16791335]
28. Liu Y, Dong X, Chen P. Chem Soc Rev. 2012; 41:2283–2307. [PubMed: 22143223]
29. Zhou W, Saran R, Liu J. Chem Rev. 2017; 117:8272–8325. [PubMed: 28598605]
30. Liu J, Cao Z, Lu Y. Chem Rev. 2009; 109:1948–1998. [PubMed: 19301873]
31. Lu Y, Liu J. Curr Opin Chem Biol. 2006; 17:580–588.
32. Xu QH, Gaylord BS, Wang S, Bazan GC, Moses D, Heeger AJ. P Natl Acad Sci USA. 2004; 101:11634–11639.
33. Cruz SMA, Girão AF, Gonçalves G, Marques PAAP. Sensors. 2016; 16:137.
34. Afaneh AT, Schreckenbach G. J Phys Chem A. 2015; 119:8106–8116. [PubMed: 26052824]
35. Zhu Y, Deng D, Xu L, Zhu Y, Wang L, Qi B, Xu C. Anal Methods. 2015; 7:662–666.
36. Liu J, Lu Y. J Am Chem Soc. 2003; 125:6642–6643. [PubMed: 12769568]
37. Yun W, Cai D, Jiang J, Zhao P, Huang Y, Sang G. Biosens Bioelectron. 2016; 80:187–193. [PubMed: 26836648]
38. Xiao Y, Rowe AA, Plaxco KW. J Am Chem Soc. 2007; 129:262–263. [PubMed: 17212391]
39. Liu J, Lu Y. J Am Chem Soc. 2007; 129:9838–9839. [PubMed: 17645334]
40. Liu M, Zhao H, Chen S, Yu H, Zhang Y, Quan X. Chem Commun. 2011; 47:7749–7751.
41. Yin BC, Ye BC, Tan W, Wang H, Xie CC. J Am Chem Soc. 2009; 131:14624–14625. [PubMed: 19824721]
42. Ge C, Luo Q, Wang D, Zhao S, Liang X, Yu L, Xing X, Zeng L. Anal Chem. 2014; 86:6387–6392. [PubMed: 24950121]
43. Li L, Luo L, Mu X, Sun T, Guo L. Anal Methods. 2010; 2:627–630.
44. Sidaginamale RP, Joyce TJ, Lord JK, Jefferson R, Blain PG, Nargol AVF, Langton DJ. Bone Joint Res. 2013; 2:84–95. [PubMed: 23836464]
45. Jantzen C, Jørgensen HL, Duus BR, Sporring SL, Lauritzen JB. Acta Orthop. 2013; 84:229–236. [PubMed: 23594249]

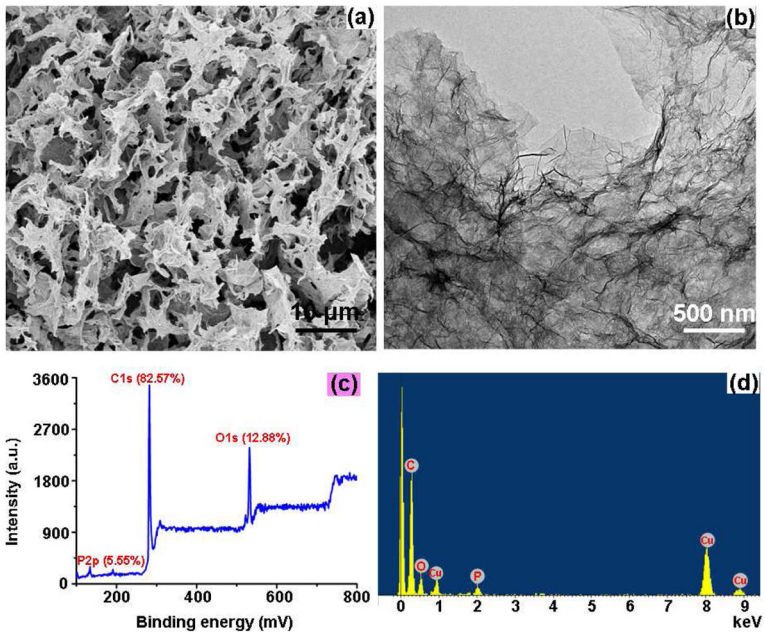

Figure 1.

a) SEM image, b) TEM image c) XPS pattern and, d) element analysis of GF.

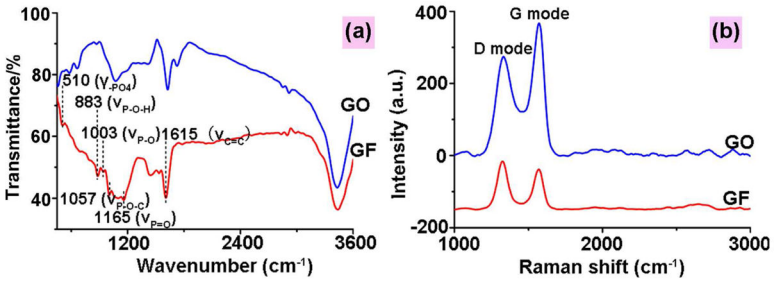

Figure 2.

a) FT-IR and b) Raman spectrum of GF.

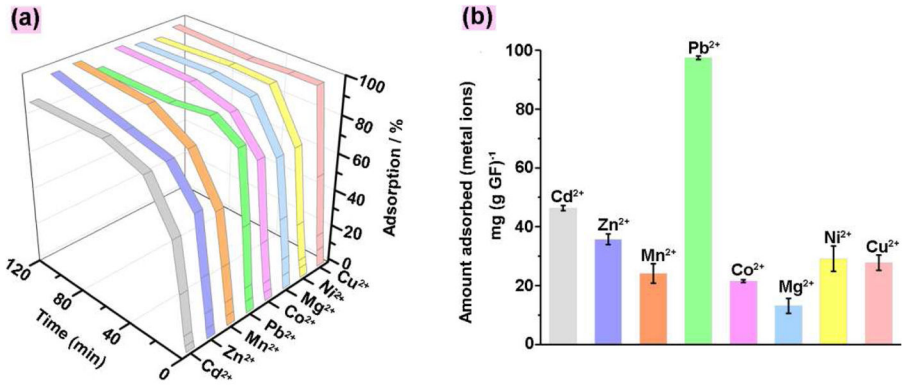

Figure 3.

a) Adsorption of metal ions in 0.5 M KCl-HCl (pH~1.5) at various incubation time; and b) the absolute amount of metal ions adsorbed by GF after 120 min in 0.5 M KCl-HCl (pH~1.5).

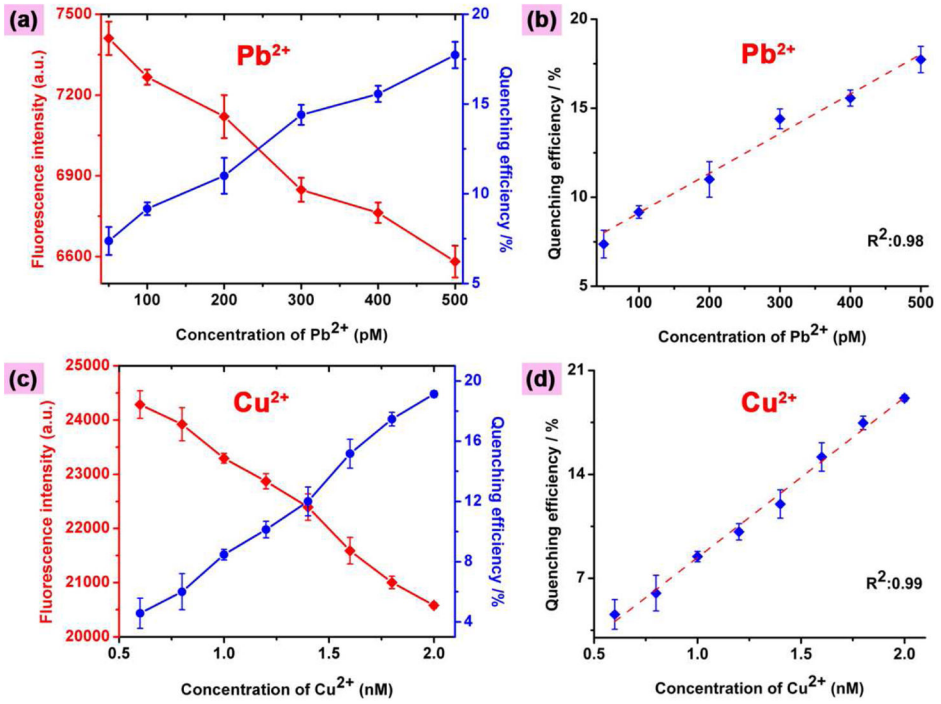

Figure 4.

a) Fluorescence response and quenching efficiency of the sensing system at different Pb^{2+} concentrations. b) Linear relationship of Pb^{2+} in concentration range from 50 to 500 pM. c) Fluorescence response and quenching efficiency of the sensing system at different Cu^{2+} concentrations. d) Linear relationship of Cu^{2+} in concentration range from 0.7 to 2.0 nM.

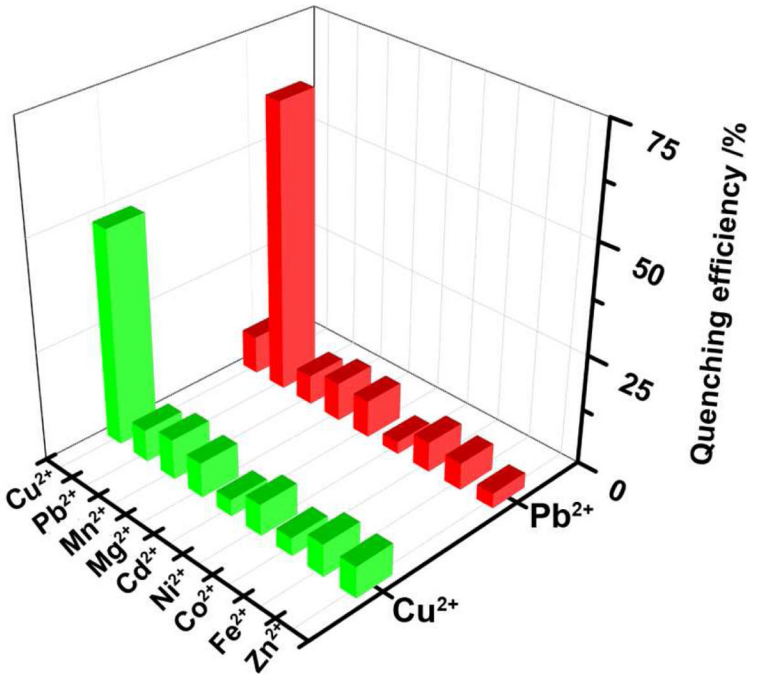

Figure 5.
Test of selectivity of the GF sensor for the simultaneous detection of Cu^{2+} and Pb^{2+}.

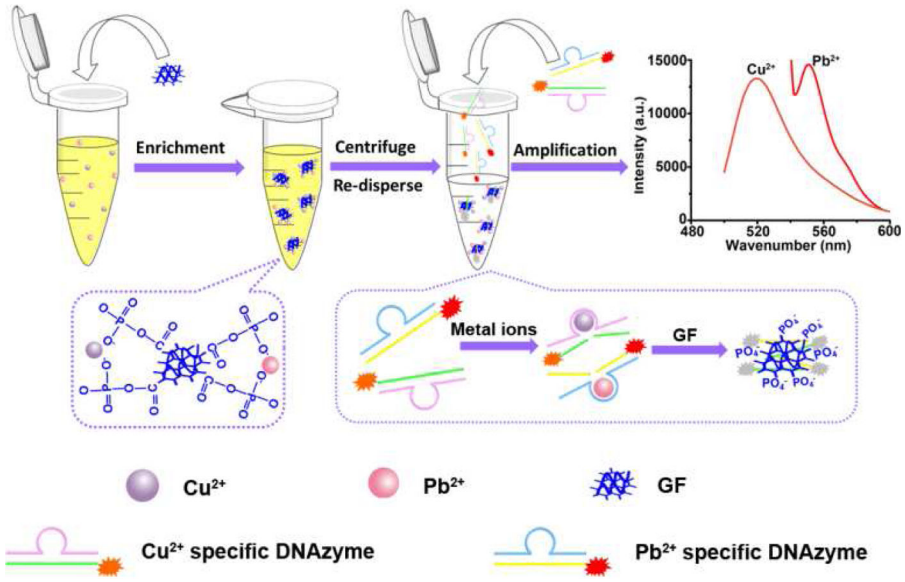

Scheme 1.

Detection of metal ions based on GF and DNAzymes.

Table 1

Limits of detection for Pb^{2+} and Cu^{2+} by various techniques.

Analyte	Technique	Output signal	LOD	Reference
Pb^{2+}	Pb^{2+}-specific DNAzyme	fluorescence	50 pM	Our design
			0.7 nM	35
		colorimetric	300 pM	19
			100 nM	36
			20 pM	37
		electrochemical	300 nM	38
Cu^{2+}	Cu^{2+}-specific DNAzyme	fluorescence	0.6 nM	Our design
			35 nM	39
		colorimetric	2 nM	40
			1 μM	41
			5.9 nM	42
		electrochemical	20 nM	43

Table 2

Determination of Cu^{2+} and Pb^{2+} in serum (n=3).

Metal ions	Spiked metal ions (nM)	Recovered metal ions (nM)	Recovery (%)
	0	<LOD	
Pb^{2+}	0.100	0.095±0.003	95.0%
	1.000	0.976±0.081	97.6%
	0	<LOD	
Cu^{2+}	1.000	0.983±0.069	98.3%
	10.000	9.776±0.132	97.8%